Supplemental Document

Biomedical Optics EXPRESS

Rapid multi-plane phase-contrast microscopy reveals torsional dynamics in flagellar motion: supplement

SOHEIL MOJIRI,[1] SEBASTIAN ISBANER,[1] STEFFEN MÜHLE,[1] HONGJE JANG,[1] ALBERT JOHANN BAE,[2] INGO GREGOR,[1] AZAM GHOLAMI,[2,3] AND JÖRG ENDERLEIN[1,*]

[1] *III. Institute of Physics – Biophysics, Georg-August-University, 37077 Göttingen, Germany*
[2] *Max-Planck-Institute for Dynamics and Self-Organization, 37077 Göttingen, Germany*
[3] *Cluster of Excellence "Multiscale Bioimaging: from Molecular Machines to Networks of Excitable Cells" (MBExC), Georg-August-University, 37077 Göttingen, Germany*
[*] *jenderl@gwdg.de*
http:www.joerg-enderlein.de

Supplement DOI: https://doi.org/10.6084/m9.figshare.14462112

Parent Article DOI: https://doi.org/10.1364/BOE.419099

Rapid multi-plane phase-contrast microscopy reveals torsional dynamics in flagellar motion: Supplementary information

Soheil Mojiri,[1] Sebastian Isbaner,[1] Steffen Mühle,[1] Hongje Jang,[1] Albert Johann Bae,[2,3] Ingo Gregor,[1] Azam Gholami,[2] Jörg Enderlein[1,4]*

[1] III. Institute of Physics – Biophysics, Georg August University, Göttingen, Germany.
[2] Max Planck Institute for Dynamics and Self-Organization, Göttingen, Germany.
[3] Department of Biomedical Engineering, University of Rochester, USA.
[4] Cluster of Excellence "Multiscale Bioimaging: from Molecular Machines to Networks of Excitable Cells" (MBExC), Georg August University, Göttingen, Germany.
* Corresponding author. Email: jenderl@gwdg.de.

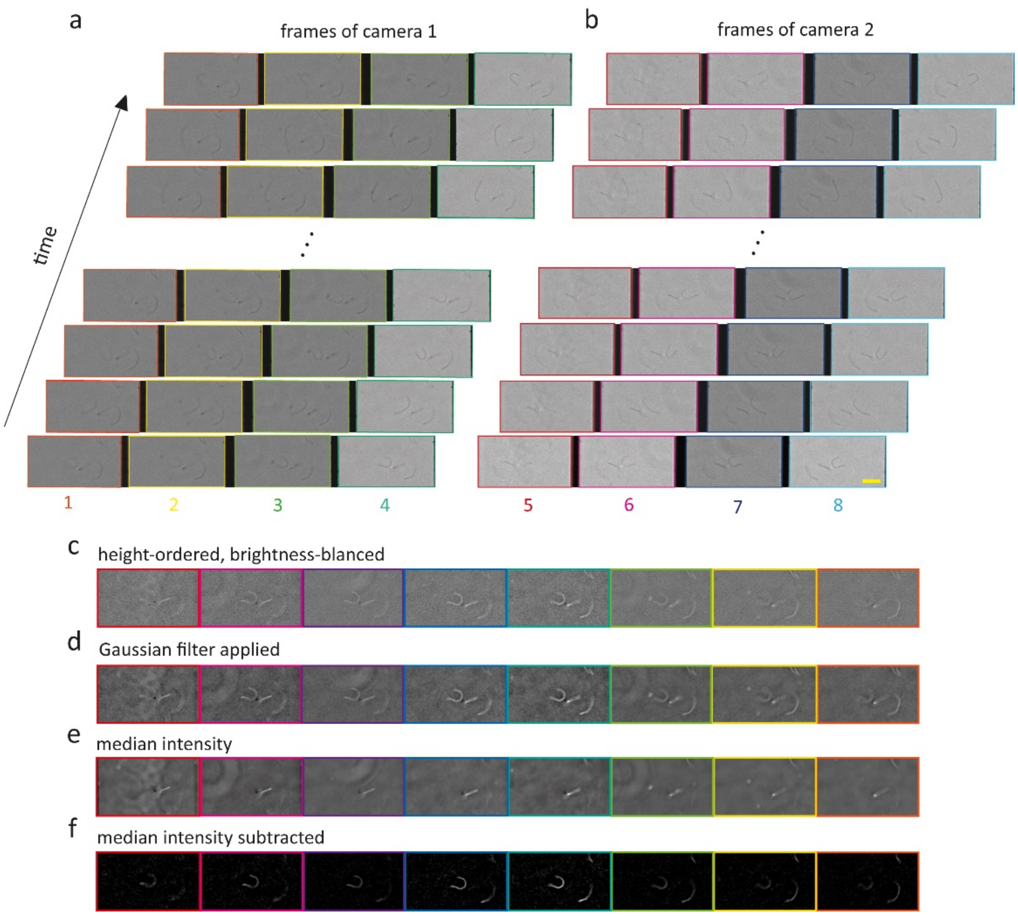

Fig. S1. Image acquisition, registering and filtering. (a,b) Four phase-contrast images acquired by camera 1 (bottom planes) and camera 2 (top planes), respectively. Length of yellow scale bar in (b) is 10 μm. **(c)** Image intensities are inverted (for better contrast) and planes are ordered following their distance from the surface, from left (bottom) to right (top). Brightness values of all planes are balanced using the ε(plane #) values from the calibration measurement. **(d)** Image noise is reduced by applying a 2D Gaussian low pass filter. **(e)** Median intensity of each plane over 1980 frames. **(f)** Subtraction of median intensity images for enhancing image contrast.

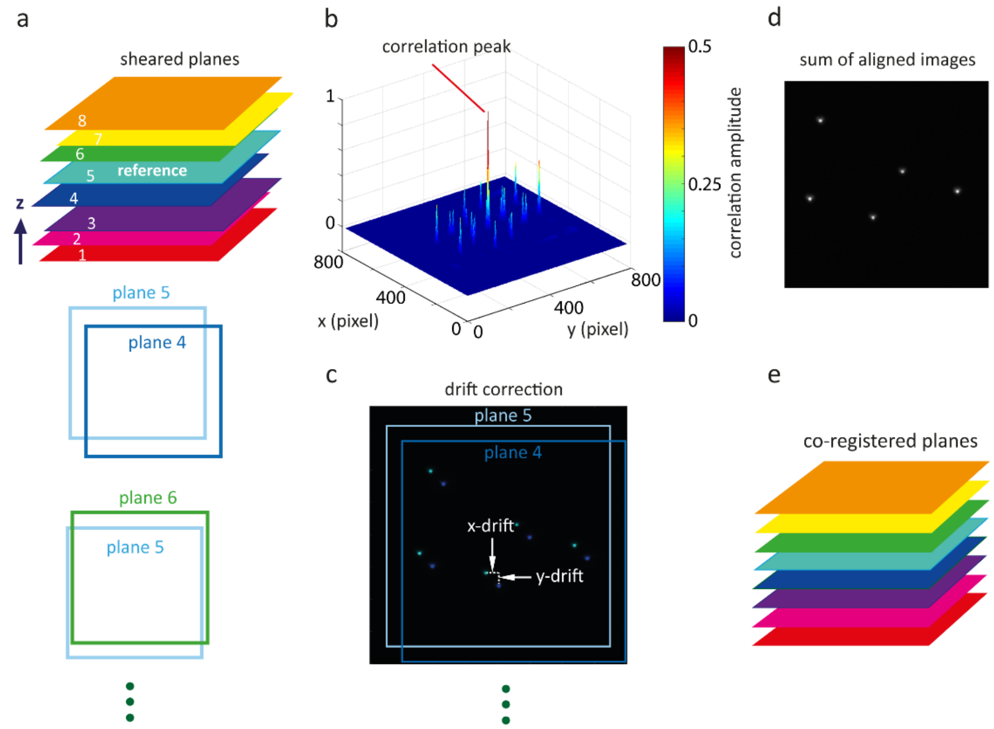

Fig. S2. Shear correction. (a) Example of plane shearing where fifth plane from bottom is considered as reference image. **(b)** Cross-correlation between one plane with reference. Peak position defines direction and value of shear between considered plane and reference plane. **(c)** Shear correction between plane 4 and 5. **(d)** Overlay of aligned planes 4 and 5. **(e)** Shear-corrected image stack of eight planes.

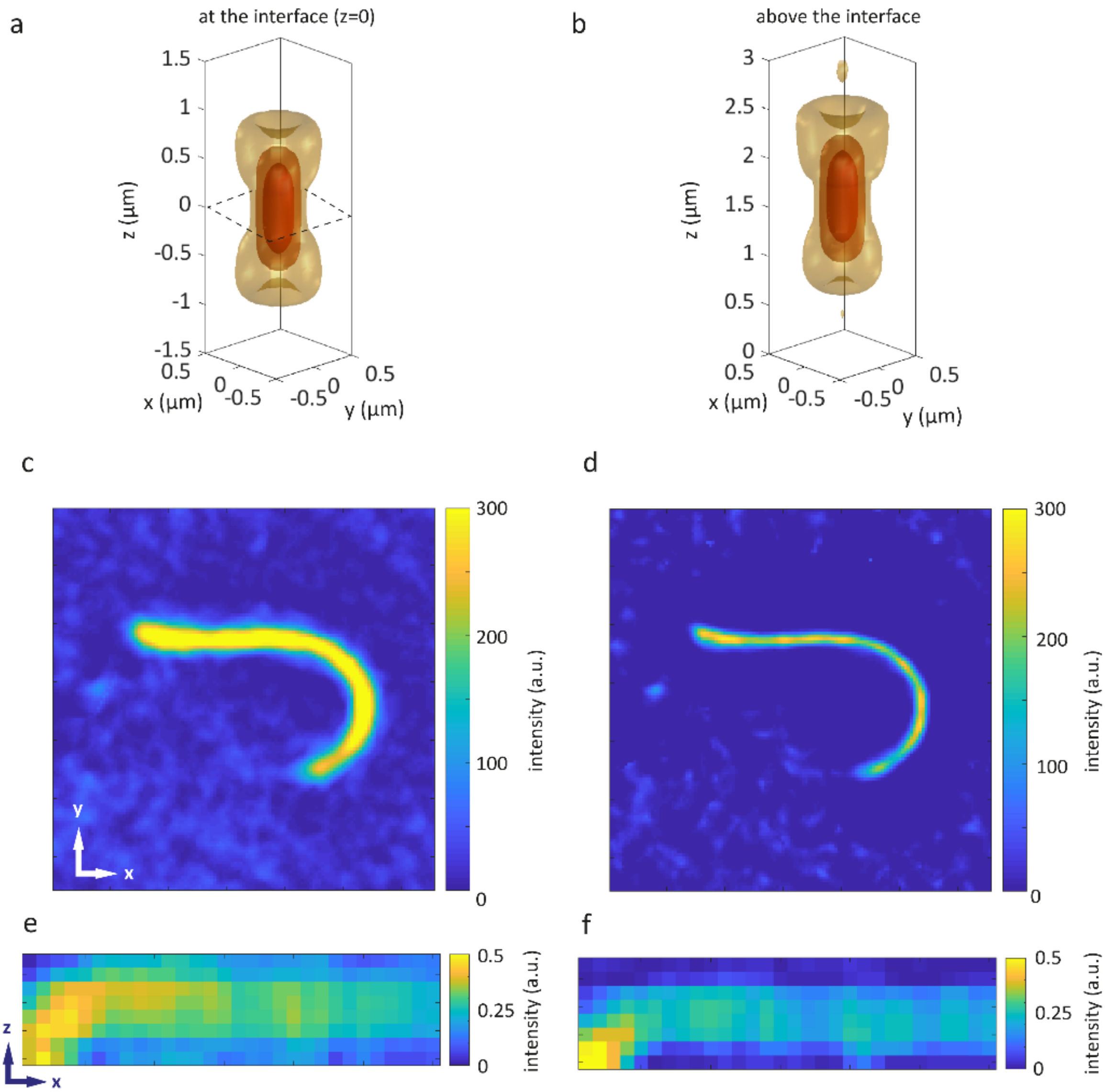

Fig. S3. Image sharpening by 3D deconvolution. (a) Iso-surfaces (at $1/e$, $1/e^2$ and $1/e^3$ of its maximum value at the center) of a calculated PSF directly at the glass-water interface (indicated by dashed line). **(b)** The same for a nominal focus position of 1.5 µm above the glass interface. Although small changes can be seen for the $1/e^3$ iso-surface, the center shape and values of the PSF are nearly identical to those of the aberration-free PSF in panel (a). **(c)** Maximum projection of axoneme image along the optical axis. **(d)** The same image after deconvolution. **(f)** Maximum projection of axoneme image along a lateral direction. **(e)** Same image after deconvolution.

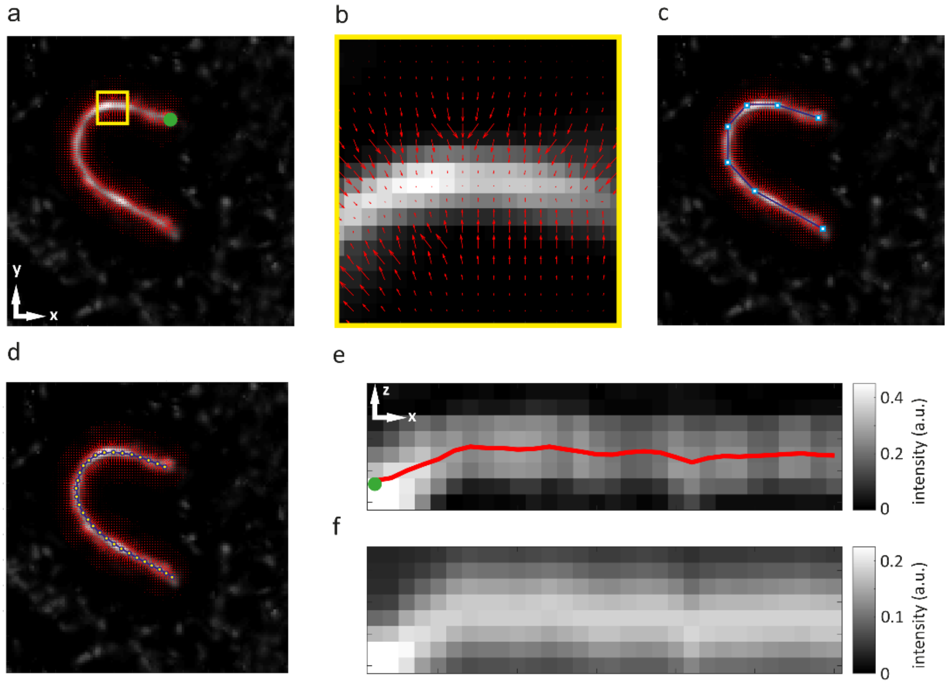

Fig. S4. 3D tracking of axonemal motion. (a) Maximum intensity projection of axoneme image (green dot indicates basal end). **(b)** Calculated vector for small yellow region of panel (a), converging toward pixels with maximum intensity. **(c)** A polygonal line with seven nodes along the contour snake. **(d)** Division of snake into 30 segments. **(e)** Vertical cross section of axonemal image and contour (green dot indicates basal end). **(f)** Same as (e), but after fitting axial intensity distribution at each lateral position with a 1D Gaussian.

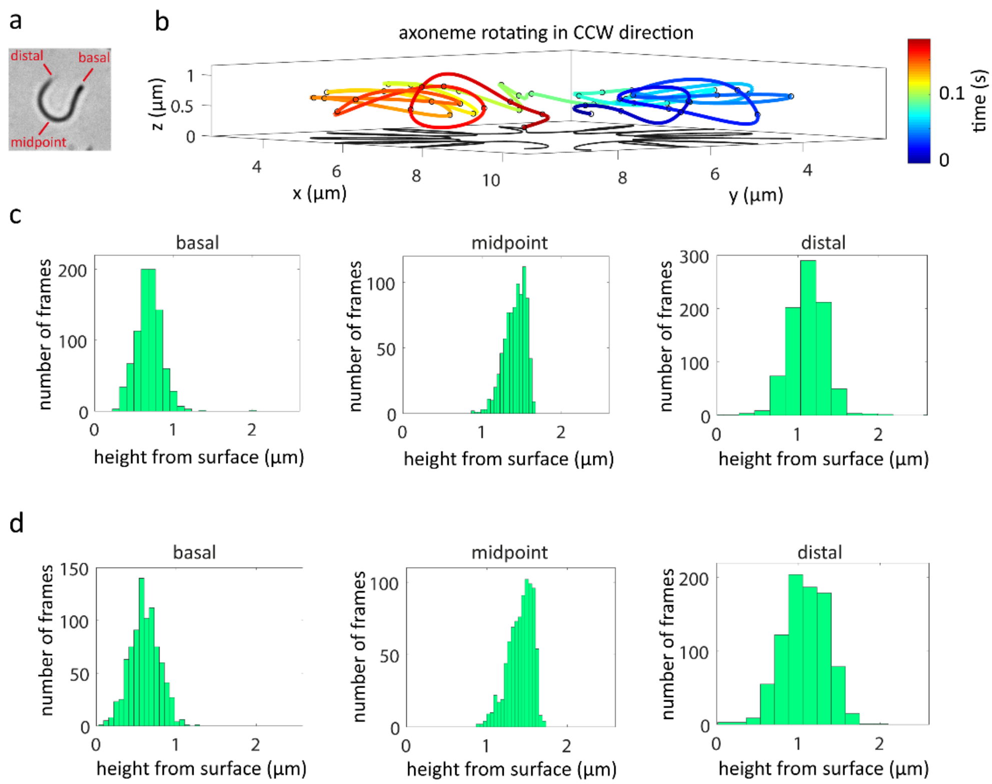

e

height from surface (nm)	basal end	midpoint	distal end
axoneme # 1	687 ± 164	1412 ± 136	1114 ± 247
axoneme # 2	603 ± 181	1417 ± 153	1082 ± 278

Fig. S5. 3D swimming trajectories. (a) 2D maximum intensity projection image of one axoneme with indication of first two segments taken as basal end (the slightly thicker end), midpoint (intermediate segments numbers 14-16), and distal end (last two segments). **(b)** Swimming trajectories of basal end over nearly one complete rotation for axoneme 1 frames (axoneme presented in Fig. 4a, b in main text). Time progress is color-coded. The black shadow at the bottom is the projection of the path on the surface. **(c)** Height distributions of basal end, midpoint, and distal end of axoneme shown in panel (b) over 860 for axoneme 1. **(d)** Same as panel (b), but for axoneme 2 (presented in Fig. 4c, d). **(e)** Table of mean values and standard deviations of the height distribution for the basal end, midpoint, and distal end in the two axonemes shown in panels (c, d).

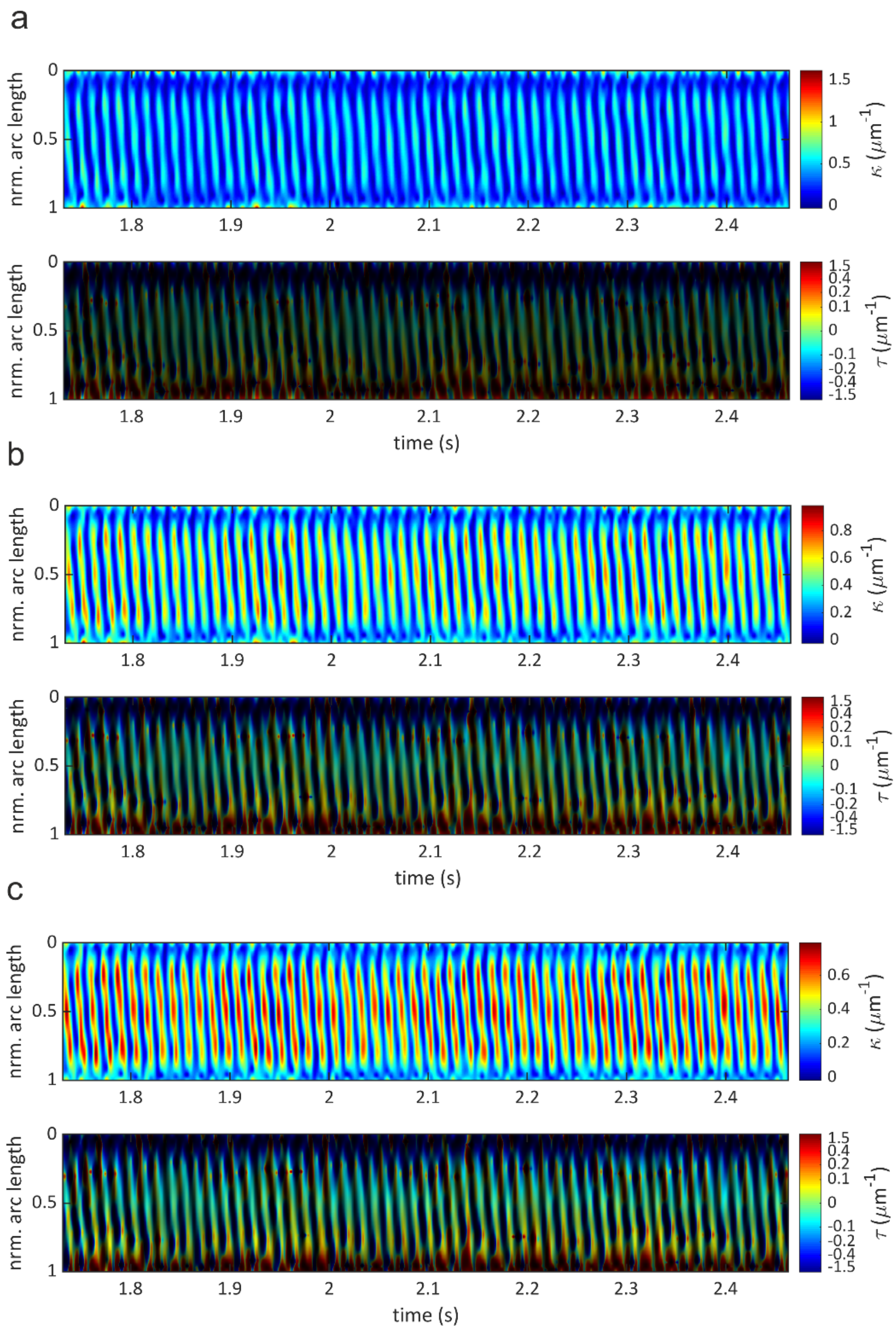

Fig. S6. Effect of contour padding on calculated curvature and torsion. (a) Zero padding, **(b)** padding with one extra point, **(c)** padding with two extra points. Compare with Fig. 4 in main text showing results for padding with three extra points. As can be seen, padding does mostly suppress excessive curvature values at contour ends, but does nearly not change curvature values elsewhere, and has little impact on torsion values (different brightness values in torsion plots are due to different dynamic range of curvature values).

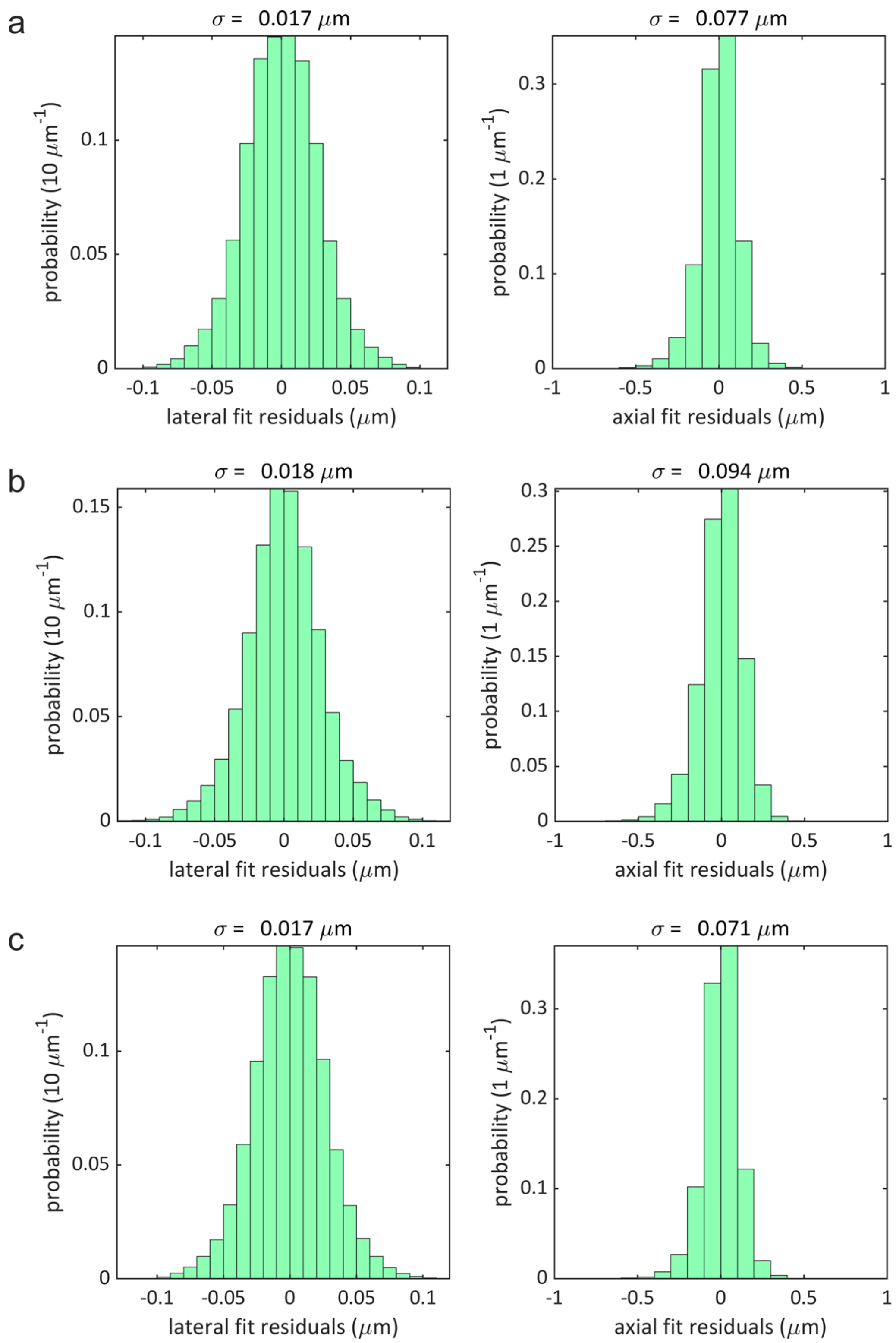

Fig. S7. Distributions of standard deviations between discretized and fitted position values. (a,b) For flagellum of Fig. 4a,b, where we used a Gaussian filter for initial image processing in (a) and a more sophisticated noise filtering method based on a windowed Fourier transform in (b), see main text for more details. Panel **(c)** shows the result for flagellum of Fig. 4c,d in main text when using a Gaussian filter. Left panels show standard deviation distributions for lateral x,y-positions, right panels for axial z-positions. Calculated standard deviation values $\sigma_{x,z}$ for all distributions are given on top of each panel.

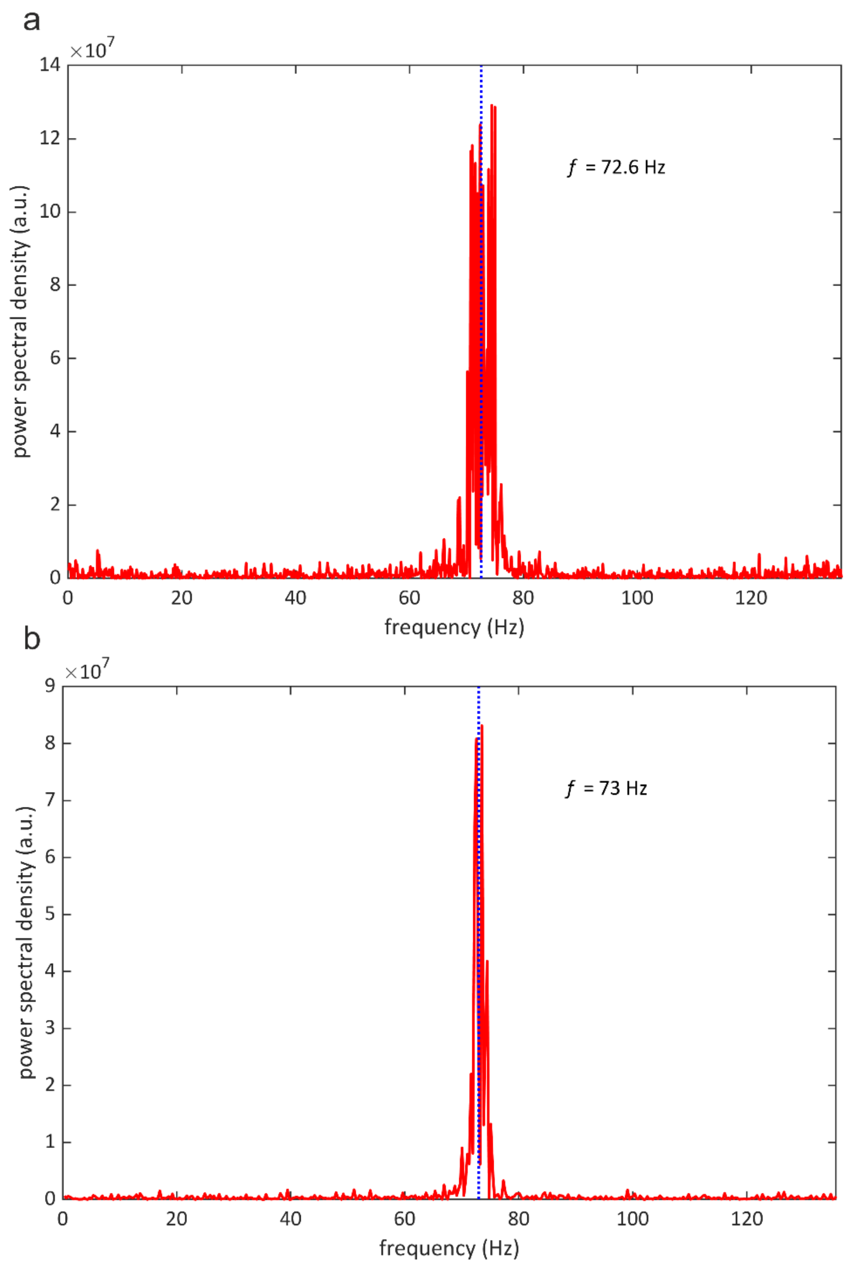

Fig. S8. Power Spectral Densities (PSDs). (a) PSD calculated from curvature values shown in Fig. 4b and **(b)** Fig. 4d in main text. PSDs are calculated as the absolute square of the temporal Fourier transform of curvature values averaged along an axoneme's contour. Dominant frequency is displayed next to each peak, corresponding to the beating frequencies of the axonemes.

Component	Details
white light source	100W 12V Halogen Lamp U-LH100L-3 (Olympus), peak wavelength in 585 nm
phase annulus	IX-PH3, 35 mm diameter (Olympus)
condenser lens	IX2-LWUCD Universal Condenser (Olympus), N.A. 0.55, W.D. 27 mm
microscope stage	ES107IX2 (Prior Scientific Instruments), 115 mm × 77 mm travel range, 1 μm step resolution, OptiScan ES107 controller
phase objective	UPLFLN 60XOIPH, 0.65-1.25 N.A. (Olympus)
tube lens	f_{TL} = 180 mm (Olympus)
field aperture	SP 40 slit (Owis)
telescope lenses	f_{L1} = 150 mm, f_{L2} = 200 mm, achromatic doublets AC254-150-A-ML, AC254-200-A-ML (Thorlabs)
multi-plane prism	Corning C-7980, n_D = 1.458, Abbe number ν = 67.8, see section 6.2 in SI of Ref.~[Descloux2018]
cameras	ORCA-Flash 4.0 V2 (Hamamatsu), pixel size = 6.5 μm

Table S1. Specifications of components incorporated into the multi plane phase-contrast microscope

Movie Video1.mp4. Three-dimensional flagellar motion and tracking. Spatio-temporal dynamics of discretized (red) and fitted (blue) contour of flagellum used in Fig. 4a,b in main text. Shown are also projections onto the three (x,y), (x,z) and (z,x) coordinate planes.

Movie Video2.mp4. Three-dimensional flagellar motion and tracking. Same as Video1, but for the flagellum used in Fig. 4c,d.